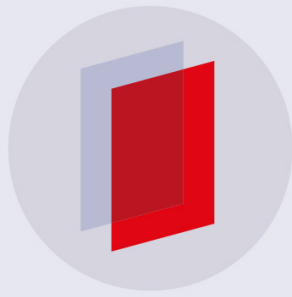


PAPER • OPEN ACCESS

## Investigation of different small-scale flux-rope acceleration scenarios for energetic particles in the solar wind near Earth

To cite this article: J A le Roux *et al* 2018 *J. Phys.: Conf. Ser.* **1100** 012015

View the [article online](#) for updates and enhancements.



**IOP** | **ebooks**<sup>TM</sup>

Bringing you innovative digital publishing with leading voices to create your essential collection of books in STEM research.

Start exploring the collection - download the first chapter of every title for free.

# Investigation of different small-scale flux-rope acceleration scenarios for energetic particles in the solar wind near Earth

**J A le Roux<sup>1,2</sup>, G P Zank<sup>1,2</sup> and O V Khabarova<sup>3</sup>**

<sup>1</sup> Department of Space Science, University of Alabama in Huntsville (UAH), 320 Sparkman Drive, AL 35805, USA

<sup>2</sup>Center of Space Plasma Science and Aeronomics Research (CSPAR), University of Alabama in Huntsville (UAH), 320 Sparkman Drive, AL 35805, USA

<sup>3</sup>Heliophysics Laboratory, Pushkov Institute for Terrestrial Magnetism, Ionosphere, and Radio Wave Propagation (IZMIRAN), Moscow, Russia

jar0013@uah.edu

**Abstract.** Our previous kinetic transport theoretical development for energetic particle acceleration by and large-scale transport through solar wind regions with numerous dynamic small-scale flux ropes in the strong guide/background field limit is further analyzed and extended. The basic flux-rope acceleration mechanisms and the issue of compressibility are further clarified by applying concepts such as magnetic curvature and shear flow to these structures. A set of new coupled focused-transport-MHD turbulence equations is presented for modeling coherent and stochastic energetic particle acceleration by small-scale flux ropes self-consistently. Furthermore, test particle coherent and stochastic acceleration rates are compared for the different flux-rope acceleration mechanisms, and stochastic acceleration and pitch-angle scattering rates for flux ropes and Alfvén waves are compared, for energetic protons at Earth.

## 1. Introduction

From recent observations near 1 AU we learned: (i) Solar wind regions near primary current sheets (the heliospheric current sheet or current sheets associated with interplanetary coronal mass ejections behind traveling shocks and corotating interaction regions) are filled with contracting and merging small-scale flux ropes with cross sections belonging to the turbulence inertial range. These structures are generated when primary current sheets undergo turbulent magnetic reconnection [1,2]. (ii) Enhanced energetic particle fluxes up to MeV energies correlate well with these flux-rope regions [1,2,3]. (iii) Dynamic small-scale flux ropes are especially efficient accelerators during strong compression [1,2]. (iv) An unprecedented number of small-scale flux ropes were identified at 1 AU using the Grad-Shafranov reconstruction approach [4]. The latter result is consistent with the common occurrence of dynamic small-scale flux ropes in the low-latitude solar wind near 1 AU as a natural development of local MHD turbulence in a high conductivity plasma with a strong guide/background field and a plasma  $\beta$  of order 1 or less [5]. In this limit, the observed formation of energetic particle power-law spectra at 1 AU can be interpreted as a consequence of flux-rope dynamics, such as



Content from this work may be used under the terms of the [Creative Commons Attribution 3.0 licence](#). Any further distribution of this work must maintain attribution to the author(s) and the title of the work, journal citation and DOI.

merging, primarily occurring in the 2D plane perpendicular to a strong guide/background field [6]. Following up on the promising idea of efficient acceleration when energetic particles interact with numerous contracting and merging small-scale flux ropes [7,8], Zank et al. and le Roux et al. developed comprehensive focused transport theories of energetic particle acceleration in a turbulent magnetized plasma containing dynamic small-scale flux ropes in the strong guide field limit [9,10].

Here, the basic small-scale flux rope acceleration mechanisms are further investigated using concepts such as magnetic curvature and the shear-flow tensor. The difference between the incompressible and compressible limits of flux-rope dynamics for acceleration, and the close link between guiding center kinetic and focused transport theory are addressed anew. An extended theory is presented for modeling self-consistent energetic particle acceleration by small-scale flux ropes. This involves coupling of the focused transport equation to a new MHD equation for total magnetic island energy density advective transport in the non-uniform solar wind medium, derived from a recent version of nearly incompressible MHD theory for solar wind turbulence [5]. The latter equation includes magnetic island damping rates derived from assuming conservation of total energy in the exchange of energy between energetic particles and magnetic islands during coherent and stochastic acceleration. Finally, for energetic protons at 1 AU, coherent and stochastic flux-rope acceleration rates for the different flux-rope acceleration mechanisms are discussed, and stochastic acceleration and pitch-angle scattering rates for flux ropes and Alfvén waves are compared.

## 2. The small-scale flux rope acceleration mechanisms

### 2.1 A Guiding center kinetic theory perspective

Small-scale flux ropes detected near Earth have cross sections of  $L \sim 0.01\text{-}0.001$  AU [1,2]. Near 1 AU, suprathermal protons, e.g., have gyro-radii  $r_g \ll L$  for a wide range of energies that easily include MeV energies. Thus, standard guiding center kinetic theory, which is restricted to gyro-radii much less than scale of the electromagnetic field in the plasma, is well suited for modeling energetic particle transport through and acceleration in solar wind regions near Earth with numerous contracting and merging small-scale flux rope structures. In guiding center kinetic theory, the gyro-phase-averaged rate of change in kinetic energy for energetic charged particles can be expressed in different ways:

$$\begin{aligned} \left\langle \frac{dK}{dt} \right\rangle_{\phi} &\approx \left[ qE \bullet \left( v_{\parallel} \underline{b} + \frac{mv_{\parallel}^2}{qB} \underline{b} \times \underline{\kappa} \right) \right]_{\parallel} + \left[ M \frac{\partial B}{\partial t} + qE \bullet \left( \frac{M}{q} \frac{\underline{B} \times \nabla B}{B^2} + \frac{M}{q} (\nabla \times \underline{b})_{\parallel} \underline{b} \right) \right]_{\perp} \\ &\approx \left[ qE_{REC\parallel} v\mu + mv^2 \mu^2 (\underline{V}_E \bullet \underline{\kappa}) \right]_{\parallel} + \left[ (1 - \mu^2) M' \left( \frac{\partial B}{\partial t} + (\underline{V}_E \bullet \nabla) B \right) + (1 - \mu^2) B \frac{dM'}{dt} \right]_{\perp} \quad (1) \\ &\approx \left[ qE_{REC\parallel} v\mu + mv^2 \mu^2 (\underline{V}_E \bullet \underline{\kappa}) \right]_{\parallel} + \left[ -mv^2 \frac{1}{2} (1 - \mu^2) [(\underline{V}_E \bullet \underline{\kappa}) + (\nabla \bullet \underline{V}_E)] \right]_{\perp} \end{aligned}$$

where  $q$  is the net particle charge,  $v_{\parallel}$  is the parallel guiding velocity component,  $\underline{b}$  is the unit vector along the flux-rope magnetic field,  $\underline{\kappa} = (\underline{b} \bullet \nabla) \underline{b}$  is the curvature of the flux-rope magnetic field,  $M$  is the magnetic moment of a gyrating particle,  $\underline{E} \bullet \underline{b} = E_{REC\parallel}$  is the parallel reconnection electric field component associated with merging flux-rope pairs,  $\mu$  is the cosine of the particle pitch angle,  $\underline{V}_E$  is the electric field drift (plasma drift) velocity (velocity at which the curved flux-rope magnetic field is contracting or merging), and  $M'$  is the magnetic moment for  $\mu = 0$ . Equation (1), 1<sup>st</sup> line, states the basic flux-rope acceleration mechanisms grouped in terms of parallel kinetic energy changes (terms in 1<sup>st</sup> square bracket) and perpendicular kinetic energy changes (terms in 2<sup>nd</sup> square bracket). The mechanisms are: (1) Parallel guiding center motion acceleration by the parallel reconnection electric field component  $E_{REC\parallel}$  generated in reconnection regions between merging neighbouring flux ropes (1<sup>st</sup> term in 1<sup>st</sup> square bracket), (2) curvature drift acceleration by the motional electric field induced by contracting or merging small-scale flux ropes (2<sup>nd</sup> term in the 1<sup>st</sup> square bracket), (3) betatron acceleration due time variations in the flux-rope magnetic field strength (1<sup>st</sup> term in the 2<sup>nd</sup> square

bracket), (4) grad- $B$  drift acceleration by the motional electric field induced by contraction and merging of flux ropes (2<sup>nd</sup> term in the 2<sup>nd</sup> square bracket) and, (5) parallel drift acceleration by  $E_{REC\parallel}$  (the last term in 2<sup>nd</sup> square bracket). Direct comparison of the terms in the 1<sup>st</sup> line of (1) with the corresponding terms in the 2<sup>nd</sup> line reveals that one can express the curvature drift acceleration term in terms of  $\underline{V}_E \bullet \underline{\kappa}$  (advection of curved flux-rope magnetic field at plasma drift velocity), and the grad- $B$  drift acceleration term in terms of  $(\underline{V}_E \bullet \underline{\nabla})B$  (advection of the perpendicular gradient in flux-rope field strength at the plasma drift velocity). This version of the grad- $B$  drift acceleration term can be combined with the betatron acceleration term into a generalized betatron acceleration expression  $M'dB/dt = M'(\partial B/\partial t + (\underline{V}_E \bullet \underline{\nabla})B)$  (1<sup>st</sup> 2 terms in 2<sup>nd</sup> square bracket in line 2) [11]. Comparison of the last terms in line 1 and line 2 indicates that approximate conservation of magnetic moment requires a small  $E_{REC\parallel}$ -value. Furthermore, comparing the terms in the 2<sup>nd</sup> square bracket in line 2 with the corresponding terms in line 3 reveals that the generalized betatron acceleration expression in line 2 can be related to a combination of the  $\underline{V}_E \bullet \underline{\kappa}$  and the  $\underline{\nabla} \bullet \underline{V}_E$ -terms, assuming approximate magnetic moment conservation (a small  $E_{REC\parallel}$ -value). Thus, generalized betatron acceleration is determined by a competition between incompressible flux-rope contraction or merging ( $\underline{V}_E \bullet \underline{\kappa} > 0$ ) and compressible contraction or merging ( $\underline{\nabla} \bullet \underline{V}_E < 0$ ). However, such a competition does not appear in the curvature drift acceleration term that depends only on  $\underline{V}_E \bullet \underline{\kappa}$ . To investigate this issue further it is useful to introduce the relationships

$$\underline{V}_E \bullet \underline{\kappa} = -\underline{b} \bullet (\underline{b} \bullet \underline{\nabla})\underline{V}_E = -\left[ b_i b_j \sigma_{ij} + \frac{1}{3}(\underline{\nabla} \bullet \underline{V}_E) \delta_{ij} \right] \quad (2)$$

where we relate the magnetic curvature advection term  $\underline{V}_E \bullet \underline{\kappa}$  to the parallel shear-flow term  $\underline{b} \bullet (\underline{b} \bullet \underline{\nabla})\underline{V}_E$  which in turn is expressed in terms of the shear-flow tensor  $\sigma_{ij}$

$$\sigma_{ij} = \frac{1}{2} \left[ \frac{\partial V_{Ei}}{\partial x_j} + \frac{\partial V_{Ej}}{\partial x_i} - \frac{2}{3}(\underline{\nabla} \bullet \underline{V}_E) \delta_{ij} \right] \quad (3)$$

using the Cauchy Stokes theorem [12]. Upon inserting (2) in the bottom line of equation (1), we get

$$\left\langle \frac{dK}{dt} \right\rangle_\phi \approx qE_{REC\parallel}v\mu - \frac{1}{3}mv^2(\underline{\nabla} \bullet \underline{V}_E) - \frac{1}{2}mv^2(3\mu^2 - 1)b_i b_j \sigma_{ij} \quad (4)$$

where the term containing  $\underline{\nabla} \bullet \underline{V}_E$  can be recognized as the standard Parker cosmic-ray transport equation term for the combination of curvature drift, grad- $B$  drift, betatron and parallel drift acceleration that collectively becomes plasma drift compression acceleration acting on the isotropic part of the particle distribution  $f_0(p)$  [13,14]. The last term in (4) can be interpreted likewise as combining parallel shear flow tensor acceleration associated with curvature drift acceleration  $(-mv^2\mu^2 b_i b_j \sigma_{ij})$  with parallel shear flow tensor acceleration associated with unified grad- $B$  drift, betatron and parallel drift acceleration  $(+mv^2 1/2(1 - \mu^2)b_i b_j \sigma_{ij})$  that collectively becomes parallel shear-flow tensor acceleration acting on the anisotropic part of the particle distribution related to the 2nd moment of the particle distribution  $f_2(p)$ . The interpretation in terms of particle anisotropy moments is made assuming a Legendre moment expansion for the energetic particle distribution that is nearly isotropic so that  $f(p) = f_0(p) + 3\mu f_1(p) + 5/2(3\mu^2 - 1)f_2(p)$ , where  $f_1(p)$  is the 1st moment and  $f_2(p)$  is the 2nd moment in the anisotropic part of the energetic particle distribution, and averaging over all  $\mu$ -values. Upon decomposing the shear flow tensor according to  $\sigma_{ij} = \sigma_{ij}^{sh} - 1/3(\underline{\nabla} \bullet \underline{V}_E) \delta_{ij}$ , where  $b_i b_j \sigma_{ij}^{sh} = 1/2(b_i b_j \partial V_{Ei} / \partial x_j + b_j b_i \partial V_{Ej} / \partial x_i) = \underline{b} \bullet (\underline{b} \bullet \underline{\nabla})\underline{V}_E$ , in (4), the result is

$$\begin{aligned} \left\langle \frac{dK}{dt} \right\rangle_{\phi} \approx & qE_{REC\parallel} v\mu - \frac{1}{3}mv^2(\nabla \bullet \underline{V}_E) + \frac{1}{3}mv^2 \frac{1}{2}(3\mu^2 - 1)(\nabla \bullet \underline{V}_E) \\ & - \frac{1}{2}mv^2(3\mu^2 - 1)\underline{b} \bullet (\underline{b} \bullet \nabla) \underline{V}_E \end{aligned} \quad (5)$$

In addition to the Parker transport compression term, there is a new compression term (3rd term in (5)). Just like the Parker compression term, this extra term also combines compression acceleration linked to curvature drift acceleration  $(+1/3mv^2\mu^2(\nabla \bullet \underline{V}_E))$  with compression acceleration associated with unified betatron, grad-B drift, and parallel drift acceleration  $(-1/3mv^21/2(1-\mu^2)(\nabla \bullet \underline{V}_E))$  to form collectively a plasma drift compression acceleration term. Different from the Parker transport compression term that acts on the isotropic part of the particle distribution  $f_0(p)$ , the new compression term acts on the anisotropic part of the particle distribution connected with  $f_2(p)$ . The last term in (5) combines parallel shear flow acceleration associated with curvature drift acceleration  $(-mv^2\mu^2\underline{b} \bullet (\underline{b} \bullet \nabla) \underline{V}_E)$  with parallel shear flow acceleration linked to unified betatron, grad-B drift, and parallel drift acceleration  $(+mv^21/2(1-\mu^2)\underline{b} \bullet (\underline{b} \bullet \nabla) \underline{V}_E)$  to form collectively a shear-flow acceleration term (reduced shear flow tensor without the compression term) that acts only on the anisotropic part of the energetic particle distribution related to  $f_2(p)$ . Upon combining the two  $\nabla \bullet \underline{V}_E$ -terms in (5), and doing the substitution  $-\underline{b} \bullet (\underline{b} \bullet \nabla) \underline{V}_E = \underline{V}_E \bullet \underline{\kappa}$ ,

$$\left\langle \frac{dK}{dt} \right\rangle_{\phi} \approx qE_{REC\parallel} v\mu - \frac{1}{2}mv^2(1-\mu^2)(\nabla \bullet \underline{V}_E) + \frac{1}{2}mv^2(3\mu^2 - 1)(\underline{V}_E \bullet \underline{\kappa}) \quad (6)$$

whereby the last line of equation (1) is recovered. In the process we gained new insight in the  $\nabla \bullet \underline{V}_E$ -term in equation (1), having determined that it can be interpreted as a combination of curvature drift acceleration with unified betatron, grad-B drift, and parallel drift acceleration acting collectively as plasma drift compression acceleration on both the isotropic and the anisotropic part of the energetic particle distribution. The  $\underline{V}_E \bullet \underline{\kappa}$ -term, on the other hand, can be viewed as a combination of curvature drift acceleration with unified betatron, grad-B drift, and parallel drift acceleration acting collectively as plasma drift shear flow acceleration only on the anisotropic part of the distribution.

## 2.2 Compressible versus incompressible flux-rope drift and betatron acceleration

Consider first the limit of incompressible flux-rope contraction or merging (in the strong guide field limit we interpret this to mean magnetic island area conservation during contraction or merging in the 2D plane perpendicular to the guide/background magnetic field) when  $0 < -\nabla \bullet \underline{V}_E \ll \underline{V}_E \bullet \underline{\kappa} = -\underline{b} \bullet (\underline{b} \bullet \nabla) \underline{V}_E > 0$ . Then, from equations (1), (5), and (6) we have

$$\begin{aligned} \left\langle \frac{dK}{dt} \right\rangle_{\phi} \approx & \left[ qE_{REC\parallel} v\mu + mv^2\mu^2(\underline{V}_E \bullet \underline{\kappa}) \right]_{\parallel} + \left[ (1-\mu^2)M' \left( \frac{\partial B}{\partial t} + (\underline{V}_E \bullet \nabla)B \right) + (1-\mu^2)B \frac{dM'}{dt} \right]_{\perp} \\ = & \left[ qE_{REC\parallel} v\mu + mv^2\mu^2(\underline{V}_E \bullet \underline{\kappa}) \right]_{\parallel} + \left[ -mv^2 \frac{1}{2}(1-\mu^2)(\underline{V}_E \bullet \underline{\kappa}) \right]_{\perp} \\ = & \left[ qE_{REC\parallel} v\mu - mv^2\mu^2\underline{b} \bullet (\underline{b} \bullet \nabla) \underline{V}_E \right]_{\parallel} + \left[ mv^2 \frac{1}{2}(1-\mu^2)\underline{b} \bullet (\underline{b} \bullet \nabla) \underline{V}_E \right]_{\perp} \end{aligned} \quad (7)$$

For magnetic island contraction or merging ( $\underline{V}_E \bullet \underline{\kappa} > 0$ ) it is clear that curvature drift acceleration must result in parallel kinetic energy gain (2nd term in 1<sup>st</sup> square bracket in (7)). However, for generalized betatron acceleration (compare 1<sup>st</sup> 2 terms in 2<sup>nd</sup> square bracket in line 1 with the term in 2<sup>nd</sup> square bracket in lines 2 and 3) the result is perpendicular kinetic energy loss, assuming approximate conservation of  $M$  (neglecting the last term in the 2<sup>nd</sup> square bracket in line 1). it means that  $M' dB/dt = M'(\partial B/\partial t + (\underline{V}_E \bullet \nabla)B) < 0$ . In this way we can relate the perpendicular energy loss to a decreasing

magnetic field strength inside flux-rope structures following the plasma drift  $\underline{V}_E$  during incompressible flux-rope contraction or merging. If in the generalized betatron expression grad- $B$  drift acceleration is negligible compared to betatron acceleration [15], perpendicular kinetic energy loss is caused by the time variation in the field strength rather than the spatial variation so that energy loss is predominantly associated with the standard betatron acceleration term  $M'(\partial B/\partial t)$ . Note that incompressible contraction or merging is associated with a negative parallel shear flow component in flux ropes ( $\underline{V}_E \bullet \underline{\kappa} = -\underline{b} \bullet (\underline{b} \bullet \nabla) \underline{V}_E > 0$ ).

In conclusion, energetic particle acceleration in incompressible contracting and merging small-scale flux ropes is related to parallel plasma drift shear flow acceleration involving a competition between parallel kinetic energy gain from curvature drift acceleration, and perpendicular kinetic energy loss predominantly from betatron acceleration. On average, the net acceleration from the combination of the two acceleration processes only involves the anisotropic part  $f_2(p)$  of the particle distribution, assuming an expansion of the distribution to the 2<sup>nd</sup> moment.

When flux-rope contraction and merging occurs in the compressible limit (area reduction during contraction or merging in 2D magnetic island plane perpendicular to the guide magnetic field) so that  $0 < -\nabla \bullet \underline{V}_E \gg \underline{V}_E \bullet \underline{\kappa} = -\underline{b} \bullet (\underline{b} \bullet \nabla) \underline{V}_E > 0$ , we find from equations (1), (5), and (6) that

$$\begin{aligned} \left\langle \frac{dK}{dt} \right\rangle_{\phi} &\approx \left[ qE_{REC\parallel} v\mu + mv^2 \mu^2 (\underline{V}_E \bullet \underline{\kappa}) \right]_{\parallel} + \left[ (1 - \mu^2) M' \left( \frac{\partial B}{\partial t} + (\underline{V}_E \bullet \nabla) B \right) + (1 - \mu^2) B \frac{dM'}{dt} \right]_{\perp} \\ &\approx \left[ qE_{REC\parallel} v\mu - mv^2 \mu^2 \frac{1}{3} (\nabla \bullet \underline{V}_E) \right]_{\parallel} + \left[ -mv^2 \frac{1}{2} (1 - \mu^2) \frac{2}{3} (\nabla \bullet \underline{V}_E) \right]_{\perp} \end{aligned} \quad (8)$$

where for simplicity compression terms acting on  $f_2(p)$  has been neglected in favour of those acting on  $f_0(p)$  (nearly isotropic particle distribution). During contraction and merging in the compressible limit  $\nabla \bullet \underline{V}_E < 0$  and, although relatively small,  $\underline{V}_E \bullet \underline{\kappa} > 0$ . Thus, the 2<sup>nd</sup> term in the 1<sup>st</sup> square bracket in both lines 1 and 2 of (8) suggests that curvature drift acceleration will contribute to parallel kinetic energy gain. By comparing the generalized betatron expression (1<sup>st</sup> two terms in the 2<sup>nd</sup> square bracket in line 1) with the term in the 2<sup>nd</sup> square bracket in line 2, it follows that the generalized betatron acceleration term will result in perpendicular kinetic energy gain ( $\nabla \bullet \underline{V}_E < 0$ ), assuming  $dM'/dt \approx 0$ . Therefore,  $M' dB/dt = M'(\partial B/\partial t + (\underline{V}_E \bullet \nabla) B) > 0$ , relating the perpendicular energy gain to an increasing magnetic field strength with time following the plasma drift flow in flux ropes contracting and merging in the compressible limit. If grad- $B$  drift acceleration is negligible compared to betatron acceleration in the generalized betatron expression, as mentioned above, the perpendicular kinetic energy gain is associated with the standard betatron acceleration term  $M'(\partial B/\partial t)$  indicating an increasing flux-rope field strength in time rather than spatially.

To summarize, in contrast to finding curvature drift energy gain and betatron energy loss associated with a negative parallel component of flux-rope shear flow during incompressible contraction or merging, we find both curvature drift and betatron energy gain associated with flux-rope flow during compressible flux-rope contraction or merging [9,10]. Furthermore, on average, net energy gain for the two acceleration processes in the incompressible limit is linked only to the anisotropic part of the energetic particle distribution, whereas net energy gain for the same two processes in the compressible limit involves both the isotropic and anisotropic part of the distribution. For a further discussion of the role of shear flow and compression in small-scale flux rope acceleration, see [16].

Consider finally the 1<sup>st</sup> term in equation (1) which is associated with parallel guiding center motion acceleration by the parallel reconnection electric field formed at the interface of merging small-scale flux ropes. In this case, the result is parallel kinetic energy gain or loss depending on whether the guiding center motion is in the direction of or in the opposite direction of the reconnection electric field force. Therefore it makes sense that, averaged over all  $\mu$ -values, net acceleration only occur for the anisotropic part of the distribution (zero net acceleration for an isotropic distribution). In this sense the acceleration has the same characteristics as parallel shear flow acceleration, but the difference is

that net acceleration in the latter case only depends on  $f_2(p)$  whereas acceleration by the parallel reconnection electric field involves  $f_1(p)$ .

### 2.3 The focused transport theory connection

We model the induced electric field in contracting and merging flux ropes as  $\underline{E}_I = -\underline{U}_I \times \underline{B}$ , where  $\underline{U}_I$  is the flux-rope plasma flow velocity. Then the contraction/merging velocity in flux ropes  $\underline{V}_E = \underline{U}_I = \underline{U}_\perp$ . Making this substitution in equations (5) and (6) reveals the close connection between standard guiding center kinetic theory and focused transport kinetic theory that we use to model particle acceleration by dynamic small-scale flux ropes because, according to focused transport theory,

$$\frac{1}{p} \left\langle \frac{dp}{dt} \right\rangle_\phi^I = \mu \left( \frac{q \underline{E}_{REC}}{p} - \frac{1}{v} \frac{d \underline{U}_I}{dt} \right) \bullet \underline{b} - \frac{1}{2} (1 - \mu^2) (\nabla \bullet \underline{U}_I) - \frac{1}{2} (3\mu^2 - 1) \underline{b} \bullet (\underline{b} \bullet \nabla) \underline{U}_I \quad (9)$$

The only difference between equations (5) and (6), and (9) is the presence of an additional acceleration term referring to parallel guiding center motion acceleration by the non-inertial force associated with the parallel component of the acceleration of the flux-rope flow  $d\underline{U}_I/dt \bullet \underline{b}$  ( $d/dt = \partial/\partial t + \underline{U} \bullet \nabla$ ).

In (9), the reconnection electric field in merging (reconnecting) flux ropes is modeled assuming that flux rope dynamics occur mainly in a 2D plane containing the magnetic island (twist) component  $\underline{B}_I$  and flow  $\underline{U}_I$  of the flux rope perpendicular to the guide field (axial) component  $\underline{B}_0$  when the guide field is strong [6]. Near Earth it appears that assuming  $B_I/B_0 \ll 1$  is reasonable [17], and furthermore there is evidence that the flux-rope guide field is aligned with the solar wind spiral magnetic field [18]. Since our focus is on large-scale transport of energetic particles through multiple flux ropes with cross sections on turbulence inertial range scales, we model the reconnection electric field on macroscopic (MHD) scales as  $\underline{E}_{REC} = -\underline{U}_I \times \underline{B}_I \parallel \underline{B}_0 \approx \underline{B}_{TOT} = \underline{B}_0 + \underline{B}_I$ . Therefore,  $\underline{E}_{REC} \approx \underline{E}_{REC\parallel}$ . In the strong guide field limit, the electric field induced by flux-rope contraction and merging is mainly in the 2D plane perpendicular to  $\underline{B}_0$ , because  $\underline{E}_I \approx -\underline{U}_I \times \underline{B}_0 \perp \underline{B}_0$ . Therefore, curvature and grad- $B$  drift acceleration occur largely in the 2D plane, while parallel guiding center motion acceleration by the parallel reconnection electric field is mainly restricted to the guide field direction. In the strong guide field limit, the magnetic field unit vector  $\underline{b}$  can be decomposed as  $\underline{b} \approx \underline{b}_0 + \underline{B}_I/B_0$ , where  $\underline{b}_0$  is the unit vector along the guide/background field. Accordingly, the flux-rope acceleration mechanisms in quasi-2D flux ropes in focused transport theory are classified as follows:

$$\frac{1}{p} \left\langle \frac{dp}{dt} \right\rangle_\phi^I = \mu (v_{REC}^I + v_{ACC}^I) + \frac{1}{2} (3\mu^2 - 1) v_{INC}^I + \frac{1}{2} (1 - \mu^2) v_{COM}^I \quad (10)$$

where

$$\begin{aligned} v_{REC}^I &= \frac{q \underline{E}_{REC} \bullet \underline{b}}{p} \approx -\frac{q}{p} \underline{U}_I \times \underline{B}_I \bullet \underline{b}_0 \\ v_{ACC}^I &= -\frac{1}{v} \frac{d \underline{U}_I}{dt} \bullet \underline{b} \\ v_{INC}^I &= -\underline{b} \bullet (\underline{b} \bullet \nabla) \underline{U}_I \approx -\frac{\underline{B}_I}{B_0} \bullet \left( \frac{\underline{B}_I}{B_0} \bullet \nabla \right) \underline{U}_I \\ v_{COM}^I &= -(\nabla \bullet \underline{U}_I) \end{aligned} \quad (11)$$

In (11) we list the approximate relative momentum rates of change (without the  $\mu$ -dependence) for the different flux-rope acceleration cases: (i)  $v_{REC}$  refers to parallel guiding center motion acceleration by the parallel reconnection electric field force generated in merging flux ropes structures, (ii)  $v_{ACC}$  denotes parallel guiding center motion acceleration by the parallel non-inertial force associated with the acceleration of the flux-rope flow, (iii)  $v_{INC}$  indicates combined curvature and generalized betatron acceleration (parallel shear-flow acceleration) when flux ropes contract and merge in the

incompressible limit ( $\underline{U}_I \bullet \underline{K} \gg |\nabla \bullet \underline{U}_I|$ ), (iv) and  $v_{COM}$  represents curvature drift and generalized betatron acceleration (compression acceleration) for flux ropes contracting and merging in the compressible limit ( $|\nabla \bullet \underline{U}_I| \gg \underline{U}_I \bullet \underline{K}$ ). The expressions in (11) also serve as approximate expressions for the rate of change of particle pitch angle (related to  $\langle d\mu/dt \rangle_\phi$  when including the  $\mu$ -dependence) induced by the different flux-rope acceleration cases. To this, focused transport theory adds the pitch-angle rate of change generated by the magnetic mirroring force acting on energetic particles in flux ropes which we express as  $v_{REF} = v(\nabla \bullet \underline{b}) \approx v(\nabla \bullet \underline{B}_I/B_0)$ .

### 3. The coupled focused-transport-MHD equations for self-consistent energetic particle acceleration by dynamic small-scale flux ropes

Using perturbation analysis involving the decomposition of the different momentum/pitch-angle variation rates as  $v_i^I = \langle v_i^I \rangle + \delta v_i^I$ , where  $\langle v_i^I \rangle$  is the mean rate and  $\delta v_i^I$  a random fluctuating rate, a focused transport equation for energetic particle interaction with numerous small-scale flux ropes was derived that models both coherent energetic particle acceleration in response to mean, and stochastic (2<sup>nd</sup> order Fermi) acceleration in response to statistical fluctuations in flux-rope dynamic properties [10]. The current version of the equation includes additional transport terms related to  $v_{ACC}$  with additional and more detailed transport coefficient expressions than before. Furthermore, based on nearly incompressible MHD theory for low-frequency solar wind turbulence [5], a new equation was derived for the transport of the energy of the quasi-2D magnetic island component of small-scale flux ropes in a non-uniform solar wind medium. Coupling between the two equations was established by deriving damping coefficients for magnetic island energy on the basis of total energy conservation in the exchange of energy between energetic particles and magnetic islands and including them in the magnetic island transport equation. The basic structure of the coupled equations is as follows:

$$\begin{aligned} \left( \frac{df}{dt} \right)_{SW} &= - \left\langle \nabla \bullet \left( \left\langle \frac{dx}{dt} \right\rangle_\phi^I (\varepsilon_I) f \right) \right\rangle - \frac{1}{p^2} \frac{\partial}{\partial p} \left( p^2 \left\langle \frac{dp}{dt} \right\rangle_\phi^I (\varepsilon_I) f \right) - \frac{\partial}{\partial \mu} \left( \left\langle \frac{d\mu}{dt} \right\rangle_\phi^I (\varepsilon_I) f \right) \\ &\quad + \frac{\partial}{\partial \mu} \left( D_{\mu\mu}^I (\varepsilon_I) \frac{\partial f}{\partial \mu} + D_{\mu p}^I (\varepsilon_I) \frac{\partial f}{\partial p} \right) + \frac{1}{p^2} \frac{\partial}{\partial p} \left( p^2 \left[ D_{p\mu}^I (\varepsilon_I) \frac{\partial f}{\partial \mu} + D_{pp}^I (\varepsilon_I) \frac{\partial f}{\partial p} \right] \right) \quad (12) \\ \left( \frac{d\varepsilon_I}{dt} \right)_{SW} &= \gamma_I^{coh}(f) \varepsilon_I + \gamma_I^{stoch}(f) \varepsilon_I \end{aligned}$$

where the energetic particle distribution is  $f(\underline{x}, p, \mu, t)$ . The top equation in (12) is an extended focused transport equation for the propagation of energetic particles through and acceleration by numerous dynamic small-scale flux ropes in the non-uniform solar wind medium. On the left hand side of this equation  $(df/dt)_{SW}$  represents the standard focused transport equation for energetic particle transport in the non-uniform solar wind flow and magnetic field [19]. On the right hand side are additional terms for modeling the interaction of energetic particles with dynamic small-scale flux ropes. This includes

$$\begin{aligned} \left\langle \frac{dp}{dt} \right\rangle_\phi^I (\varepsilon_I) &= p \left[ \frac{1}{2} (1 - \mu^2) \langle v_{COM}^I \rangle (\varepsilon_I) + \frac{1}{2} (3\mu^2 - 1) \langle v_{INC}^I \rangle (\varepsilon_I) \right] \\ &\quad + p \left[ \mu \left( \langle v_{REC}^I \rangle (\varepsilon_I) + \langle v_{ACC}^I \rangle (\varepsilon_I) \right) \right] \quad (13) \end{aligned}$$

which is the average, coherent energetic particle momentum rate of change in response to mean flux-rope properties for all the flux-rope acceleration cases, and

$$D_{pp}^I(\varepsilon_I) = p^2 \left\langle \left[ \frac{1}{2}(1-\mu^2)\delta\nu_{COM}^I(\varepsilon_I) + \frac{1}{2}(3\mu^2-1)\delta\nu_{INC}^I(\varepsilon_I) + \mu(\delta\nu_{REC}^I(\varepsilon_I) + \delta\nu_{ACC}^I(\varepsilon_I)) \right]^2 \right\rangle \tau_{dec} \quad (14)$$

is the momentum diffusion coefficient associated with the variance in the momentum rate of change for all the flux-rope acceleration mechanisms (stochastic acceleration) in response to fluctuations in flux-rope dynamic properties [20], and  $\tau_{dec}$  is the energetic particle decorrelation time, the time scale on which propagating particles see decorrelated magnetic island properties. The expression for this time scale depends on the assumed model for particle propagation for which two limits, the quasi-linear and the non-linear transport limits, can be specified in our theory depending on the strength of the island magnetic field [10,21]. In the quasi-linear limit, decorrelation for energetic particles occurs through undisturbed guiding center motion, whereas in the non-linear transport limit decorrelation is realized in terms of assumed diffusive guiding center motion predominantly in the guide/background field direction (scattering on smaller magnetic islands produced in a forward cascade). Viewed on large scales, both transport limits manifest as parallel diffusion of energetic particles across numerous flux-rope structures mainly along the guide field, found to be an important element for more efficient acceleration in 3D simulations of particle acceleration by dynamic flux ropes [22]. In the presence of strong energetic particle scattering, as might occur in strong turbulence conditions behind heliospheric shocks, coherent particle acceleration by flux ropes becomes stochastic, resulting in additional momentum diffusion coefficient expressions for 2<sup>nd</sup> order Fermi acceleration that can be derived by taking the diffusion approximation limit (not shown) [8,9,10].

In equation (12), the bottom equation models the transport of the total energy density  $\varepsilon_I$  (kinetic plus magnetic) of the magnetic island component of small-scale flux ropes. On the left hand side of this transport equation  $(d\varepsilon_I/dt)_{SW}$  is given by

$$\begin{aligned} \frac{\partial \varepsilon_I}{\partial t} + \nabla \cdot (\varepsilon_I \underline{U}_0) + \frac{1}{2} \left[ 1 + (4a-1)\sigma_D^I \right] (\nabla \cdot \underline{U}_0) \varepsilon_I \\ - \frac{1}{4} \left[ (1+\sigma_C^I)^{3/2} - (1+\sigma_C^I)^{1/2} \sigma_D^I + (1-\sigma_C^I)^{3/2} - (1-\sigma_C^I)^{1/2} \sigma_D^I \right] \left[ \frac{2^{1/2}}{\rho_0^{3/2}} (n \cdot \nabla) \rho_0 \right] \varepsilon_I^{3/2} \\ + \frac{\left( 1 - (\sigma_C^I)^2 \right)^{1/2}}{L_I} \left[ (1+\sigma_C^I)^{1/2} + (1-\sigma_C^I)^{1/2} \right] \left[ \frac{2}{\rho_0} \right]^{1/2} \varepsilon_I^{3/2} \end{aligned} \quad (15)$$

where  $\underline{U}_0$  is the background solar wind flow velocity,  $a = 1/2$  indicates that, statistically, quasi-2D magnetic island energy is distributed axisymmetrically around  $\underline{B}_0$ ,  $\sigma_C^I$  is the normalized cross helicity and  $\sigma_D^I$  is the normalized residual energy associated with magnetic island turbulence [5],  $\rho_0$  is the background solar wind density, and  $\underline{n}$  is a unit vector pointing in an arbitrary direction along magnetic island turbulence in the 2D plane perpendicular to  $\underline{B}_0$ . Equation (15), which models the transport of  $\varepsilon_I$  in the non-uniform background solar wind medium, was derived from the quasi-2D magnetic island turbulence equations in Elsässer variables in nearly incompressible MHD theory for turbulence in a solar wind with plasma  $\beta \sim 1$ , thus making it suitable for application in the supersonic solar wind flow near Earth [5]. An interesting aspect of this equation is that in the advection term (2<sup>nd</sup> term in (15)),  $\underline{U}_0$  is present, but not the Alfvén speed, indicating that magnetic island structures are advected with the solar wind. The 3<sup>rd</sup> and 4<sup>th</sup> terms in equation (15) describe how large-scale solar wind flow compression and a large-scale density gradient in the solar wind, respectively, can enhance the energy density of magnetic islands structures. The last term models how magnetic island energy density is reduced by a forward cascade of energy during non-linear interactions of magnetic islands. On the right hand side in the bottom equation of (12),  $\gamma_I^{coh}(f)$  represents the damping rate of magnetic island

energy density when energetic particles experience coherent acceleration by small-scale flux ropes, and  $\gamma_I^{stoch}(f)$  models the damping rate of magnetic island energy density when energetic particle are stochastically accelerated by small-scale flux ropes. The expressions of these damping coefficients are given by

$$\begin{aligned}\gamma_I^{coh}(f) &= -\frac{1}{2\pi} \frac{1}{\varepsilon_I} \int_{-1}^1 d\mu \int_0^\infty dp p^2 v \left\langle \frac{dp}{dt} \right\rangle_\phi^I (\varepsilon_I) f \\ \gamma_I^{stoch}(f) &= \frac{1}{2\pi} \frac{1}{\varepsilon_I} \int_{-1}^1 d\mu \int_0^\infty dp p^2 v \left( D_{p\mu}^I(\varepsilon_I) \frac{\partial f}{\partial \mu} + D_{pp}^I(\varepsilon_I) \frac{\partial f}{\partial p} \right)\end{aligned}\quad (16)$$

These expressions, derived assuming total energy conservation in the energy exchange between energetic particles and small-scale flux ropes, enable us to model energetic particle acceleration by numerous small-scale flux ropes in a self-consistent fashion. This extension of the theory was motivated by test particle solutions for energetic particle acceleration by small-scale flux ropes that generated power-law spectra with high particle pressure [9,10]. It is interesting to note that whereas  $\gamma_I^{stoch}(f)$  depends on the pitch-angle and momentum gradients of the energetic particle distribution as we are accustomed to in quasi-linear kinetic theories,  $\gamma_I^{coh}(f)$  depends only on the particle distribution function itself. The pitch-angle gradient  $\partial f / \partial \mu$  can potentially also result in growth in magnetic island energy density.

#### 4. Comparing coherent flux-rope acceleration mechanisms at Earth

Based on our focused transport theory for energetic particle acceleration discussed above, we derived expressions for the average coherent momentum gain rate ratios for the different flux-rope acceleration cases listed in equation (11). The expressions for energetic ions are

$$\begin{aligned}\frac{\langle dp / dt \rangle_{\phi,\mu}^{INC}}{\langle dp / dt \rangle_{\phi,\mu}^{COM}} &\approx \frac{\langle v_{INC}^I \rangle}{\langle v_{COM}^I \rangle} \frac{3f_2(p)}{f_0(p)} = \frac{\sigma_{INC}^I}{\sigma_{COM}^I} \frac{\langle \delta B_I^2 \rangle}{B_0^2} \frac{3f_2(p)}{f_0(p)} \\ \frac{\langle dp / dt \rangle_{\phi,\mu}^{REC}}{\langle dp / dt \rangle_{\phi,\mu}^{COM}} &\approx \frac{\langle v_{REC}^I \rangle}{\langle v_{COM}^I \rangle} \frac{3f_1(p)}{f_0(p)} = \frac{\sigma_{INC}^I}{\sigma_{COM}^I} \frac{Z}{A} \frac{L_I}{d_i} \frac{V_{A0}}{v} \frac{\langle \delta B_I^2 \rangle^{1/2}}{B_0} \frac{3f_1(p)}{f_0(p)} \\ \frac{\langle dp / dt \rangle_{\phi,\mu}^{REC}}{\langle dp / dt \rangle_{\phi,\mu}^{INC}} &\approx \frac{\langle v_{REC}^I \rangle}{\langle v_{INC}^I \rangle} \frac{f_1(p)}{f_2(p)} = \frac{\sigma_{INC}^I}{\sigma_{INC}^I} \frac{Z}{A} \frac{L_I}{d_i} \frac{V_{A0}}{v} \frac{B_0}{\langle \delta B_I^2 \rangle^{1/2}} \frac{f_1(p)}{f_2(p)}\end{aligned}\quad (17)$$

The derivation of these expressions includes (i) the weighting factor of a nearly isotropic particle distribution, modeled by expanding it up to the 2<sup>nd</sup> moment in terms of a Legendre polynomial expansion with respect to  $\mu$ , as discussed above, and, (ii) averaging the expressions over all  $\mu$ -values. In (17),  $\langle \delta B_I^2 \rangle / B_0^2$  is the ratio of the average magnetic field energy density of the magnetic island component over the magnetic field energy density of the guide/background field component of small-scale flux ropes,  $V_{A0}$  is the Alfvén speed of the background solar wind,  $L_I$  is the flux-rope cross section,  $d_i$  is the ion inertial scale length,  $Z/A$  is the ratio of the ion atomic number over the mass number, and  $\sigma_i^I, i = INC, COM, REC, ACC$ , represents control parameters for the efficiency of coherent acceleration for the different flux-rope acceleration cases.

Consider the ratio of the coherent acceleration rate of combined curvature and generalized betatron acceleration (unified betatron and grad-B drift acceleration) in contracting and merging small-scale flux ropes operating in the incompressible limit  $\langle dp / dt \rangle_{\phi,\mu}^{INC}$  (shear-flow acceleration) to the coherent

acceleration rate for the same acceleration mechanisms in the compressible limit  $\langle dp/dt \rangle_{\phi,\mu}^{COM}$  (adiabatic compression acceleration) in the 1<sup>st</sup> line of (14). Assuming  $\sigma_{INC}^I / \sigma_{INC}^I \approx 1$ , and that at 1 AU, small-scale flux ropes with cross sections in the inertial range are in the strong guide field limit ( $\langle \delta B_I^2 \rangle / B_0^2 \approx 0.1$  [17]), we find that  $\langle dp/dt \rangle_{\phi,\mu}^{INC} / \langle dp/dt \rangle_{\phi,\mu}^{COM} \approx 0.1 \ll 1$  if we assume that the expression holds for a significant energetic particle anisotropy  $3f_2(p)/f_0(p) \approx 1$ . However, one would expect near-isotropic energetic particle distributions to exist in the enhanced turbulence conditions behind heliospheric shocks, for example. For a small anisotropy,  $\langle dp/dt \rangle_{\phi,\mu}^{INC} / \langle dp/dt \rangle_{\phi,\mu}^{COM} \ll 0.1$ . In the extreme limit of a purely isotropic particle distribution ( $f_2(p) = 0$ ),  $\langle dp/dt \rangle_{\phi,\mu}^{INC} = 0$ . This points to a key difference alluded to above that coherent shear-flow acceleration by incompressible flux ropes only yields net acceleration when the particle distribution is anisotropic whereas coherent flux-rope compression acceleration produces net acceleration for both isotropic and anisotropic particle distributions. In the limit of a strictly isotropic distribution, no net shear-flow acceleration associated with incompressible flux-rope contraction and merging indicates that the probability for parallel kinetic energy gain from curvature drift acceleration equals the probability for perpendicular kinetic energy loss from generalized betatron acceleration [8,9,10].

In conclusion, in the test particle limit, coherent energetic ion acceleration at Earth involving combined curvature and generalized betatron acceleration in quasi-2D contracting and merging small-scale flux ropes operating in the compressible limit is estimated to be much more efficient compared to when the same acceleration mechanisms occur in small-scale flux ropes acting in the incompressible limit. Equivalently, compression acceleration is predicted to be much more efficient than shear-flow acceleration. This conclusion holds as long as the anisotropic part of the particle distribution does not strongly dominate the isotropic part of the distribution. According to (17), what is required for shear-flow acceleration in incompressible flux ropes to rival compression acceleration in compressible flux ropes would be to maintain a particle anisotropy on the level  $3f_2(p)/f_0(p) \approx 1$ , combined with a weaker guide field so that  $\langle \delta B_I^2 \rangle / B_0^2 \approx 1$ . There is evidence from kinetic particle simulations that, for a guide field of approximately this strength, the energetic particle anisotropy can be sufficiently large so that shear-flow and compression acceleration reach a comparable level of efficiency [16].

Based on the above analysis, one could ask whether there is any reason to expect flux-rope dynamics in the solar wind to be in the compressible limit when the strong guide field limit applies. Although it appears that small-scale flux ropes tend to contract predominantly incompressibly in discussions of particle simulations with a significant guide field [16], and also is thought of as intrinsically incompressible in its manifestation as the quasi-2D turbulence component of coherent structures in nearly incompressible MHD theory of solar wind turbulence [5], there is observational evidence to the contrary. For example, when primary current sheets associated with interplanetary coronal mass ejections (ICMEs) interact with the heliospheric current sheet, the current sheets are disturbed and several small-scale flux rope structures may be formed when turbulent magnetic reconnection occur in these structures. The flux ropes, being trapped between the converging heliospheric current sheet and the primary current sheets of ICMEs, experience compression which may lead to efficient particle acceleration by compressing flux ropes [1,2]. Furthermore, in nearly incompressible MHD theory of quasi-2D magnetic island turbulence, incompressible flux ropes can become compressible under the influence of large-scale density and flow velocity gradients gradients in the non-uniform solar wind [5]. For example, the flow compression across heliospheric shocks might result in the emission of compressible small-scale flux ropes [23]. Closer to the Sun, Guidoni et al. [24] discusses the possibility of strong plasma compression during magnetic island contraction for islands propagating sunward during a solar flare event.

Next, we analyze the ratio of the coherent parallel guiding center motion acceleration rate due to the mean parallel reconnection electric field in merging small-scale flux ropes  $\langle dp/dt \rangle_{\phi,\mu}^{REC}$  to the coherent acceleration rate of combined curvature and generalized betatron acceleration in small-scale flux ropes contracting and merging in the compressible limit  $\langle dp/dt \rangle_{\phi,\mu}^{COM}$  (2<sup>nd</sup> line of (17)). Overall,  $\langle dp/dt \rangle_{\phi,\mu}^{REC} / \langle dp/dt \rangle_{\phi,\mu}^{COM} \gg 1$  at Earth for energetic protons, even though we assume the strong guide field limit  $\langle \delta B_I^2 \rangle / B_0^2 \approx 0.1$  at Earth, because of the large ratio of  $L_I/d_i$  (maximum values for  $L_I \approx 0.01$  AU and  $d_i \approx 6 \times 10^{-7}$  AU). The domination of  $\langle dp/dt \rangle_{\phi,\mu}^{REC}$  is reduced significantly at higher particle speeds because  $\langle dp/dt \rangle_{\phi,\mu}^{REC} / \langle dp/dt \rangle_{\phi,\mu}^{COM} \propto V_{A0} / v$ , but not sufficiently to affect the domination of  $\langle dp/dt \rangle_{\phi,\mu}^{REC}$ . However, if we extend the scope of the analysis by considering all flux-rope cross sections belonging to the turbulence inertial range ( $\sim 0.01$  AU  $< L_I < \sim 6 \times 10^{-7}$  AU at Earth), we find that  $\langle dp/dt \rangle_{\phi,\mu}^{COM} / \langle dp/dt \rangle_{\phi,\mu}^{REC} > 1$  for energetic protons above  $\sim 1$  keV when  $L_I < \sim 10^{-4}$  AU even if  $3f_1(p)/f_0(p) \approx 1$ . Domination by  $\langle dp/dt \rangle_{\phi,\mu}^{COM}$  can be achieved for suprathermal protons for all cross sections in the inertial range if we specify a sufficiently smaller particle anisotropy  $3f_1(p)/f_0(p) \approx 0.01$ . Assuming a purely isotropic particle distribution ( $f_1(p) = 0$ ), there is no net particle acceleration by the mean parallel reconnection electric field ( $\langle dp/dt \rangle_{\phi,\mu}^{REC} = 0$ ) because there is an equal probability for particle motion along and opposite to the mean parallel reconnection electric field force as discussed above. In summary, in the strong guide field limit applicable at 1 AU, coherent parallel guiding center motion acceleration by the mean parallel reconnection electric field due to flux-rope merging tend to be more efficient than combined curvature drift and generalized betatron acceleration in compressible flux ropes for the largest flux-rope cross sections in the inertial range, but compression acceleration by flux ropes can dominate for all cross sections in the inertial range if the energetic particle anisotropy is sufficiently small.

Consider the ratio  $\langle dp/dt \rangle_{\phi,\mu}^{REC} / \langle dp/dt \rangle_{\phi,\mu}^{INC}$  (3<sup>rd</sup> line of (17)). We find that  $\langle dp/dt \rangle_{\phi,\mu}^{REC} / \langle dp/dt \rangle_{\phi,\mu}^{INC} > 1$  for suprathermal protons at Earth for all flux-rope cross sections belonging to the inertial range when applying the strong guide field limit and limiting the particle anisotropy to  $f_1(p)/f_2(p) \approx 1$ . Domination by the parallel reconnection electric field is further strengthened for a small energetic particle anisotropy  $f_2(p)/f_1(p) \ll 1$ . A way for  $\langle dp/dt \rangle_{\phi,\mu}^{INC}$  to rival the efficiency of ( $\langle dp/dt \rangle_{\phi,\mu}^{REC} = 0$ ) for at least the smallest flux-rope cross sections in the inertial range would be to maintain a sufficiently strong particle anisotropy  $f_1(p)/f_2(p) \approx 1$  combined with a weaker guide field so that  $\langle \delta B_I^2 \rangle / B_0^2 \approx 1$  which, qualitatively, is in agreement with kinetic simulation results [16].

Coherent energetic particle parallel guiding center motion momentum gain by the mean non-inertial force associated with the parallel acceleration of the flux-rope flow  $\langle dp/dt \rangle_{\phi,\mu}^{ACC}$  (expression not shown) appears to be less efficient than momentum gain from both parallel guiding center motion momentum gain by the mean parallel reconnection electric field and combined curvature drift and generalized betatron acceleration in compressible flux ropes, and this is even more so in the case of a nearly isotropic particle distribution. Also in this case, there is no net coherent acceleration when the energetic particle distribution is strictly isotropic.

Based on our estimates for coherent energetic proton acceleration in response to mean flux-rope dynamic properties, which were made in the strong guide field limit and for flux-rope cross sections in the inertial range at 1 AU, we conclude that the two most efficient acceleration scenarios involve

combined curvature drift and generalized betatron acceleration in contracting and merging flux ropes in the compressible limit, and parallel guiding center motion acceleration by the parallel reconnection electric field of merging flux ropes. The latter tends to dominate for the largest magnetic island cross sections in the inertial range when the anisotropy in the particle distribution not too small.

### 5. Stochastic acceleration by small-scale flux ropes

A main factor that contributes to differences between the efficiency of coherent acceleration in response to mean flux-rope properties, and the efficiency of stochastic acceleration due to fluctuations in flux-rope properties, is the anisotropy in the energetic particle distribution. In the case of stochastic acceleration, both the isotropic and anisotropic part of the distribution function plays a role in all four acceleration scenarios. As discussed above, net coherent acceleration only occurs for the anisotropic part of the particle distribution for most acceleration cases. The exception is acceleration by flux-rope flow compression which also yields net acceleration when acting on the isotropic part of the distribution. We find for stochastic acceleration that all four acceleration cases contribute to particle acceleration when the particle anisotropy is strictly zero, as long as we take the quasi-linear transport limit of our theory. In the non-linear transport limit the acceleration expressions becomes undetermined in this limit. When comparing ratios of coherent acceleration rates with ratios of stochastic acceleration rates, the results are similar qualitatively for the most part. Quantitative differences in the acceleration ratios are most noticeable when near-isotropic energetic particle distributions are assumed, which is a disadvantage for most coherent acceleration scenarios.

### 6. Comparing stochastic acceleration by small-scale flux-ropes and Alfvén waves

We find that stochastic acceleration involving parallel guiding center motion acceleration of suprathermal protons at 1 AU in response to fluctuations in the parallel reconnection electric field of merging small-scale flux ropes to be the only flux-rope acceleration scenario in the quasi-linear spatial transport limit of our theory that is more effective than stochastic acceleration by parallel propagating Alfvén waves in standard quasi-linear theory [25]. However, stochastic acceleration by active small-scale flux ropes in the non-linear transport regime of our kinetic transport theory is significantly more efficient when compared to the quasi-linear limit of our theory. Consequently, in the non-linear limit also combined stochastic curvature drift and generalized betatron acceleration in response to fluctuations in the properties of small-scale flux ropes contracting and merging in the compressible limit, is more effective than stochastic acceleration by Alfvén waves for a wide range of suprathermal proton kinetic energies above  $\sim 10$  keV. The enhanced acceleration efficiency can be attributed to the fact that, in the non-linear transport regime of our theory, energetic particles are modeled to have diffusively distorted guiding center trajectories inside flux ropes (scattering on smaller-scale flux ropes) when traversing these structures in the background/guide field direction. Thus, energetic particles spend more time being accelerated in each active flux rope (quasi-trapped) compared to the quasi-linear regime. In the quasi-linear regime, particles traverse flux ropes in the guide field direction more rapidly because of the assumption of undisturbed guiding center motion, leaving less time for acceleration in each flux rope.

### 7. Pitch-angle scattering by small-scale flux-ropes and Alfvén waves

In our current focused transport approach, the variance in the magnetic mirroring force present in small-scale flux ropes is predicted to play an important role in energetic particle pitch-angle scattering in solar wind conditions at 1 AU. This is related to our finding that energetic particle pitch-angle scattering by small-scale flux ropes in the quasi-linear spatial transport limit of our focused transport theory approach is more efficient compared to previous quasi-linear kinetic theories for particle interaction with 2D turbulence, where particle scattering is determined by the variance in the magnetic Lorentz force associated with 2D turbulence. Another difference is that in earlier approaches the particle decorrelation time is determined by a competition between the time scales for gyromotion around  $\underline{B}_0$  and the turbulence dynamic time scale [e.g., 26]. Because the turbulence was treated as

strictly 2D, the option exercised in our current theory of particles experiencing decorrelated flux-rope turbulence while propagating along the guide field was not considered. In addition, we find that energetic proton pitch-angle scattering by small-scale flux ropes at 1 AU should be more efficient than pitch-angle scattering by Alfvén waves, provided that the non-linear spatial transport limit of our theory is applicable, but less efficient than pitch-angle scattering by Alfvén waves when we take the quasi-linear limit of our theory. This raises the question which limit of our theory applies best to solar wind conditions near 1 AU. Fits to observed intensity time profiles of solar energetic events at 1 AU using focused transport theory suggest that the energetic ion parallel mean free path  $\lambda_{\parallel}$  can vary widely between  $\sim 2 \times 10^{-2}$  - 1 AU during quiet solar wind conditions in the absence of interplanetary shocks [27]. Nonetheless, it appears that  $\lambda_{\parallel} > L_1$  because the maximum small-scale flux-rope cross section at 1 AU is  $L_1 \approx 0.01$  AU, indicating scatter-free transport of energetic particles through these structures so that the quasi-linear limit of our theory is more appropriate in quiet solar wind conditions. However, one would expect that the values of  $\lambda_{\parallel}$  in the enhanced turbulence levels behind traveling shocks should be significantly smaller, providing potential conditions for the application of the non-linear transport limit of our theory.

## 8. Summary

It was discussed how the basic small-scale flux rope drift and betatron acceleration mechanisms present in guiding center kinetic theory relate to flux-rope plasma drift contraction or merging in both the incompressible and compressible limits. It was shown that drift and betatron acceleration in flux-ropes undergoing incompressible contraction and merging can be interpreted in terms of shear flow acceleration linked to a negative parallel component of shear flow inside flux ropes. Drift and betatron acceleration in flux-ropes contracting and merging in the compressible limit can be viewed as compression acceleration in flux ropes with a relatively negligible magnetic curvature or parallel component of shear flow. We found that when the drift and betatron acceleration mechanisms in guiding center kinetic theory are expressed in term of plasma drift compression and shear flow acceleration, a close link exists between the flux-rope acceleration mechanisms of guiding center kinetic theory and those in focused transport theory which we use to model energetic particle acceleration by small-scale flux ropes. Focused transport theory includes an additional acceleration mechanism associated with parallel guiding center motion acceleration by the parallel component of the acceleration of the flux-rope flow (non-inertial force). Furthermore, it was discussed that, only in the case of compression acceleration, net energetic particle acceleration occurs for both the isotropic and anisotropic parts of the energetic particle distribution. For all other flux-rope acceleration scenarios (shear-flow acceleration during incompressible contraction and merging, parallel guiding center motion acceleration by the parallel reconnection electric field in merging flux ropes and the parallel component of the acceleration of the flux-rope flow (non-inertial force)), net acceleration occurs only for the anisotropic part of the distribution.

In an extension of previous work, we presented the outline of a statistical transport theory for self-consistent energetic particle acceleration by and large-scale transport through numerous contracting and merging quasi-2D small-scale flux ropes. The theory applies to flux rope cross-sections belonging to the inertial range of turbulence and is valid for small-scale flux ropes in the strong guide/background field limit. It was assumed that flux-rope dynamics are occurring essentially in the 2D plane of the magnetic island (twist) component perpendicular to the guide field (axial) component of these structures. The extended theory, as presented, consisted of two coupled equations: (i) a focused transport equation which divide all flux-rope acceleration mechanisms into coherent acceleration in response to mean magnetic island dynamic quantities, and stochastic (2<sup>nd</sup> order Fermi) acceleration due to statistical fluctuations in these quantities and, (ii) a new equation for the transport of total energy density (kinetic and magnetic) of magnetic islands advected with the non-uniform solar wind flow based on a recent nearly incompressible MHD theory for solar wind turbulence. Coupling between the two equations were established with the inclusion of newly derived magnetic island damping coefficients in the magnetic island transport equation derived on the basis of conservation of

total energy in the energy exchange between energetic particles and magnetic islands for both coherent and stochastic acceleration.

Test particle, coherent energetic proton acceleration rates at Earth were compared for different flux-rope acceleration cases in the strong guide field limit for flux-rope cross sections in the inertial range. We found the two most efficient acceleration scenarios to be combined curvature drift and generalized betatron acceleration in contracting and merging flux ropes in the compressible limit (compression acceleration), and parallel guiding center motion acceleration by the parallel reconnection electric field in merging flux ropes. The latter tended to dominate for the largest magnetic island cross sections in the inertial range provided that the anisotropy in the particle distribution not too small.

Stochastic flux-rope acceleration rates were also investigated. A key difference between the two types of acceleration is that both the isotropic and anisotropic parts of the distribution function contribute to net acceleration for all acceleration cases during stochastic acceleration. Coherent acceleration is solely determined by the anisotropic part of the particle distribution for all the acceleration cases except acceleration by flux-rope flow compression which also yields net acceleration from the isotropic part of the distribution. Comparison of stochastic acceleration for small-scale flux ropes and parallel-propagating Alfvén waves (standard quasi-linear theory) revealed that parallel guiding center motion acceleration by the parallel reconnection electric field in merging flux ropes was more efficient than Alfvén waves in the quasi-linear transport limit of our theory. In the non-linear transport regime of our theory, combined stochastic curvature drift and generalized betatron acceleration in flux ropes contracting and merging in the compressible limit (compression acceleration) can also be more efficient than stochastic acceleration by Alfvén waves for energetic protons at 1 AU.

Finally, our theory suggested that the variance in the magnetic mirroring force present in small-scale flux ropes plays a potential important role in energetic particle pitch-angle scattering in solar wind conditions at 1 AU. Analysis of pitch-angle scattering showed that energetic proton pitch-angle scattering by small-scale flux ropes should be more efficient than pitch-angle scattering by Alfvén waves, provided that the non-linear spatial transport limit of our theory is applicable, but less efficient than pitch-angle scattering by Alfvén waves when we take the quasi-linear limit of our theory.

### Acknowledgments

le Roux and Zank acknowledge support from NASA grant NNX15AI65G, and NSF-DOE grant PHY-1707247.

### References

- [1] Khabarova O V, Zank G P, Li G, le Roux J A, Webb G M, Dosch A and Malandraki O E 2015 *Astrophys. J.* **808** 181
- [2] Khabarova O V, Zank G P, Li G, Malandraki O E, le Roux J A and Webb G M 2016 *Astrophys. J.* **827** 122
- [3] Khabarova O V, Zank G P 2017 *Astrophys. J.* **843** 4
- [4] Zheng J, Hu Q 2018 *Astrophys. J.* **852** L23
- [5] Zank G, Adhikari L, Hunana P, Shiota D, Bruno R and Telloni D 2017 *Astrophys. J.* **835** 147
- [6] Dmitruk P, Matthaeus W H and Seenu N 2004 *Astrophys. J.* **617** 667
- [7] Drake J F, Swisdak M, Che H and Shay M A 2006 *Nature* **443** 553
- [8] Drake J, Swisdak M and Fermo R 2013 *Astrophys. J.* **763** L5
- [9] Zank G P, le Roux J A, Webb G M, Dosch A and Khabarova O V 2014 *Astrophys. J.* **797** 28
- [10] le Roux J A, Zank G P, Webb G M and Khabarova O V 2015 *Astrophys. J.* **801** 112
- [11] Dahlin J T, Drake J F and Swisdak M 2016 *Phys. Plasmas* **23** 120704
- [12] le Roux J A, Webb G M 2012 *Astrophys. J.* **764** 104
- [13] Kóta J 1977 *Proc. 15<sup>th</sup> Cosmic Ray Conf.*, Povdiv, Bulgaria, MG-4
- [14] Webb G M, Martinic M J and Moraal H 1981, *Proc. 17th Int. Cosmic Ray Conf.*, Paris, France, **10** 109

- [15] Pritchett P 2008 *Phys. Plasmas* **15** 102105
- [16] Li X, Guo F, Li H and Birn J 2018 *Astrophys. J.* **855** 80
- [17] Smith C W, Isenberg P A, Matthaeus W H and Richardson J D 2016 *Astrophys. J.* **638** 508
- [18] Zheng J and Hu Q 2018 *Astrophys. Lett.* **852** L23
- [19] Isenberg P A 1987 *J. Geophys. Res.* **92** 1067
- [20] Bian N H and Kontar, E P 2013 *Phys. Rev. Lett.* **110** 151101
- [21] le Roux J A, Zank G P, Webb G M and Khabarova O V 2016 *Astrophys. J.* **827** 47
- [22] Dahlin J T, Drake J. F. and Swisdak M 2017 *Physics of Plasmas* **24** 092110
- [23] Karimabadi H, Roytershteyn V, Vu H X, Omelchenko Y A, Scudder J, Daughton W, Dimmock A, Nykyri K, Wan M, Sibeck D, Tatineni M, Majumdar A, Loring B and Geveci B 2014 *Phys. Plasmas* **21** 062308
- [24] Guidoni S E, DeVore C R, Karpen J T, Lynch B J 2016 *Astrophys. J.* **820** 60
- [25] Schlickeiser R 1989 *Astrophys. J.* **336** 243
- [26] le Roux J A and Webb G M 2007 *Astrophys. J.* **667** 930
- [27] Dröge W 2005 *Adv. Space Res.* **35** 532